Available online at www.sciencedirect.com
SCIENCE DIRECT
International Journal of Pharmaceutics 320 (2006) 157–164
INTERNATIONAL JOURNAL OF PHARMACEUTICS
www.elsevier.com/locate/ijpharm

Pharmaceutical Nanotechnology

Formulation of sustained release nanoparticles loaded with a tripentone, a new anticancer agent

A. Malzert-Fréon [a,*], S. Vrignaud [a], P. Saulnier [b], V. Lisowski [c], J.P. Benoît [b], S. Rault [a]

[a] *Centre d'Etudes et de Recherche sur le Médicament de Normandie, UPRES EA 3915, Département de Pharmacie Galénique, 5 rue Vaubénard, 14032 Caen Cedex, France*
[b] *Inserm U646 Ingénierie de la Vectorisation Particulaire, 10 rue André Boquel, 49100 Angers, France*
[c] *Laboratoire des Aminoacides, Peptides et Protéines (UMR-CNRS 5810), Faculté de Pharmacie, 15 Avenue Charles Flahault, 34093 Montpellier Cedex 5, France*

Received 4 January 2006; received in revised form 4 April 2006; accepted 13 April 2006
Available online 24 May 2006

Abstract

The purpose of the present work is to develop nanoparticles of a new antitubulin agent of the family of tripentones by means of a phase inversion process. Dynamic light scattering, transmission electron microscopy and ζ-potential measurements were used to characterize tripentone loaded nanoparticles. From interfacial tension measurements and from the study of the rheological interfacial properties of the tripentone at the Labrafac®–Solutol® interface, the fraction of tripentone initially present in Labrafac® would stay in the oily core of nanocapsules. Moreover, the interpenetration of some tripentone molecules within the surfactant units helps to the stabilization of the formulated nanoparticles. The encapsulation efficiency was determined by high performance liquid chromatography (HPLC) and was found to be above 95%. In vitro release studies were carried out in blank nanoparticles containing phosphate buffer, pH 7.4, at 37 °C. The drug release kinetics was measured by HPLC. Antiproliferative activity studies on L1210 cells showed that the cytotoxic activity of tripentone was totally recovered after encapsulation of the antitubulin agent in lipid nanoparticles. This study shows that lipid nanocapsules could be a promising and effective carrier for tripentone delivery in the treatment of cancers.
© 2006 Elsevier B.V. All rights reserved.

Keywords: Tripentones; Lipid nanoparticles; Interfacial tension measurements; Cytotoxic activity

1. Introduction

Ovarian carcinomas are the most common cause of death by gynaecological cancer in women (Ziller et al., 2004; Jemal et al., 2005). By applying the current standard therapy consisting of a surgical cytoreduction followed by chemotherapy with a combination of platinum (cisplatin or carboplatin) and taxane (paclitaxel or docetaxel), an initial complete clinical response is seen in about 70% of patients (Barnes et al., 2002; Ozols et al., 2004). However, median survival is only about 3 years and the majority of women treated will recur within the first 2 years following their initial diagnosis (Mc Guire and Markman, 2003). In ovarian cancer, tumors initially appear responsive to chemotherapy, but the frequent acquired resistance results in treatment failure (Ozols et al., 2004; Ziller et al., 2004).

Recently, a new series of antitubulin agents named tripentones has been synthesized (Rault et al., 1998; Lisowski et al., 2001). Among them, a 3-(3-hydroxy-4-methoxyphenyl)-8H-thieno[2,3-*b*]pyrrolizin-8-one has shown a significant human cancer cell growth inhibitory activity in the nanomolar range over a large panel of tumoral cell lines, and in particular over resistant tumoral ovarian cells (Lisowski, 2002; Lisowski et al., 2004). A flow cytometric study has shown that L1210 cells treated by this compound were arrested in the G_2/M phases of the cell cycle with a significant percentage of cells having reinitiated a cycle of DNA synthesis without cell division (Lisowski et al., 2001, 2004). Unfortunately, this high cytotoxic activity was not recovered in vivo, probably due to a poor solubility of the tripentone in biological fluids (Lisowski et al., 2004).

To overcome the lack of drug in vivo availability, a strategy consists in associating such an hydrophobic drug with nanopar-

* Corresponding author. Tel.: +33 2 31 56 60 18; fax: +33 2 31 56 60 20.
E-mail address: aurelie.malzert-freon@unicaen.fr (A. Malzert-Fréon).

0378-5173/$ – see front matter © 2006 Elsevier B.V. All rights reserved.
doi:10.1016/j.ijpharm.2006.04.007

ticles (Brigger et al., 2002). Indeed, the use of nanoparticles (NP) for controlled delivery of anticancer agents allows the enhancement of their therapeutic efficiency (Feng and Chien, 2003). Moreover, the use of colloidal drug carriers enables sensitive therapeutically active molecules protection against in vivo degradation, patient comfort increase by avoiding repetitive bolus injection or the use of perfusion pumps, as well as better drug pharmacokinetics (Gref et al., 1995).

It has been established that passive targeting of solid neoplasms by systemically drug carriers administration can be achieved if particles present long-circulating properties and adequate particle size for optimal extravasion at tumoral sites, i.e. in the range of 50–200 nm (Hoarau et al., 2004).

Recently, lipid nanocapsules with a core–shell structure were developed according to a new solvent-free formulation process, based on the inversion phase of an emulsion (Heurtault et al., 2000, 2002a). Constituted of medium chain triglycerides (core) and hydrophilic/lipophilic surfactants (shell), their structure is a hybrid between polymeric nanocapsules and liposomes. Such nanocapsules present a stable monodisperse size distribution and their diameter can be well-controlled in the range of 20–100 nm (Heurtault et al., 2003). NP were found to be good candidates as novel carriers for hydrophobic drugs (Lamprecht et al., 2002, 2004). Moreover, it was shown that NP exhibit a relatively long half disappearance time after i.v. injection in rats (Cahouet et al., 2002). Thus, these nanocapsules could be good candidates for the formulation of tripentone nanocarriers.

The aim of the present work is to establish the feasibility of such formulation. Therefore, we determined the affinity of the drug for compounds used in the formulation process by carrying out surface tension measurements with a pendant drop method. Moreover, nanoparticles charged in tripentone were characterized in terms of size, surface potential, encapsulation efficiency, drug release and the antiproliferative activity of the encapsulated drug was estimated against a cell line model.

2. Materials and methods

2.1. Materials

The lipophilic Labrafac CC (caprylic–capric acid triglycerides) was kindly provided by Gattefosse S.A. (Saint-Priest, France). The Lipoid® S75-3 (soybean lecithin at 69% phosphatidylcholine and 10% phosphatidylethanolamine), and the Solutol® HS-15 (70% polyethylene glycol 660 hydroxystearate and 30% free polyethylene glycol 660) were gifts from Lipoid GmbH (Ludwigshafen, Germany) and BASF AG (Ludwigshafen, Germany), respectively. NaCl, methanol and acetonitrile of HPLC analytical grade were provided by Carlo Erba (Val de Reuil, France). Water was purified by passing through an elgastat option 3 water purification unit (ELGA). The tripentone (3-(3-hydroxy-4-methoxyphenyl)-8H-thieno[2,3-*b*]pyrrolizin-8-one) (Fig. 1) was synthesized according to the process previously described (Lisowski et al., 2004). The tripentone is present as orange powder; the compound is not thermosensitive in the conditions used in the study (fusion temperature of 209 °C).

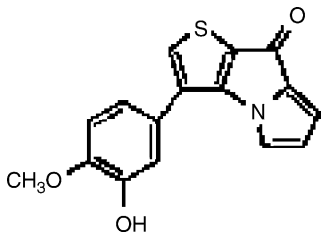

Fig. 1. Chemical structure of the tripentone studied, the 3-(3-hydroxy-4-methoxyphenyl)-8H-thieno[2,3-*b*]pyrrolizin-8-one.

2.2. Interfacial tension measurements

Interfacial tension measurements were carried out by using a Drop Tensiometer (Tracker®, ITConcept, Longessaigne, France). The apparatus has been described previously (Malzert et al., 2002a). The computer calculates up to 20 times per second the characteristic parameters of the drop (surface area, volume and surface tension) according to the Laplacian equation applied to the profile of a rising drop of Labrafac® ($d = 0.945$) in an aqueous Solutol® solution (0.1 M; $d = 0.994$). Movements of the piston of the syringe are controlled by a stepping motor connected to a microcomputer. It is thus possible to compress or expand the surface of the drop within a few percents, and to maintain the drop surface area constant during the experiments, so that the surface tension variation is related only to the adsorption of the molecules at the interface. The adsorption kinetics of the tripentone were studied at the Labrafac®–aqueous Solutol® solution (0.1 M) interface from Labrafac® [Trip.L] or from the Solutol® solution [Trip.S]. Prior to interfacial studies, tripentone was dissolved in the corresponding phase under gentle stirring, and by heating to 85 °C, at concentrations similar to those used in the formulation of nanocapsules charged with 5 mg of drug. The water used in these studies was ultrapure water, and was obtained from a Millipore® system (Milli-Q Plus 185, Molsheim, France).

2.3. Rheological measurement

Theoretical aspects have been largely developed and discussed in previous papers (Boury et al., 1995; Saulnier et al., 2001; Malzert et al., 2002b; Tewes and Boury, 2005). To summarize, the analysis of the dynamic response of interfacial films to a controlled dilatational strain (drop compression) allowed us to estimate, according to a generalized Maxwell model (Panaiotov et al., 1996), the viscoelastic parameters of the interfacial films, Ee, Ene and τ. Ee, the conservative part of the dilatational elasticity, is significant for the lateral interactions between segments of macromolecules in the plane of the interface and relevant of the rigidity of the interfacial film. Ene, the dissipative part of the dilatational elasticity, is related to molecular reorganization like expulsion of molecular chains upon compression and interactions of molecules with the adjacent liquid phase molecules. τ, the characteristic time of relaxation, represents the necessary time for the interface to reach a new equilibrium energetic state after the perturbation. In a pure elastic behavior (Ene = 0), Ee is

determined as follows:

$$\mathrm{Ee} = -A_i \frac{\mathrm{d}\gamma}{\mathrm{d}A} \quad (1)$$

2.4. Formulation of lipid nanoparticles

The preparation of NP was based on a phase inversion process (Heurtault et al., 2002a). All components (Lipoid® S75-3: 0.0375 g, lipophilic Labrafac® CC: 0.514 g, Solutol® HS-15: 0.423 g, NaCl: 0.0445 g and water: 1.281 g) were mixed and heated under magnetic stirring from ambient temperature to 85 °C, above the phase transition temperature (ca. 70 °C). The mixture was cooled down to 60 °C and the o/w nanoemulsion obtained was again heated above the phase inversion zone to give a w/o system. This cycle was repeated twice and the o/w emulsion was quenched by the addition of 3 ml cold water (0 ± 1 °C). The NP suspension was stirred for 10 min before use. In case of drug loaded NP, 5 mg of tripentone was mixed with other compounds at the beginning of the experiment, and then, the same process as the one for blank particles was applied.

2.5. Nanoparticle characterization

2.5.1. Measurement of particle size and size distribution

The average hydrodynamic particle radius (R_h) and the polydispersity index (PDI) of the NP were estimated by dynamic light scattering (DLS) using a Malvern-ALV HPPS (Malvern Instruments S.A., Worcestershire, UK), and fitted with a 632.8 nm laser beam at a fixed angle of 173° at 25 °C. A 1:10 dilution of the NP suspension in distilled water (in order to assure a convenient scattered intensity on the detectors), and a filtration of all batches through 0.2 μm syringe filters (Supelco Minisart plus filters, Sigma–Aldrich, Saint-Quentin Fallavier, France) were achieved before measurements. Data were analyzed according to the cumulants and the Contin methods. In the cumulants method, the electric field autocorrelation function is expanded in terms of the distribution moments of the decay rates. In the Contin method, a direct numerical inversion (Laplace inversion) of the intensity correlation function is made (Maulucci et al., 2005).

2.5.2. Measurement of the ζ-potential

The ζ-potential measurements were performed using a Malvern Zetasizer 3 (Malvern Instruments S.A.). A 1:100 dilution of the NP suspension in NaCl 1 mM was performed and measurements were made in triplicate at 25 °C, with a dielectric constant of 79, a refractive index of 1.33, a viscosity of 0.89 cP, 150 V cell voltage and a current of 5 mA.

2.5.3. Morphology

Transmission electron microscopy (TEM) analysis was performed using a JEOL 1011 instrument (JEOL, Croissy/Seine, France) (150 kV) in order to determine the shape of the produced nanoparticles. Before analysis, the NP dispersions were stained by a cationic negative stain (2% uranyl acetate aqueous solution), and sprayed onto copper grids overlayed with 1% formwar in chloroform.

2.5.4. Encapsulation efficiency

The drug entrapped in the nanocapsules was determined in triplicate by HPLC (Waters Alliance 2695, Waters, Saint-Quentin en Yvelines, France). A reverse phase X Terra MSC18 column (5 cm × 2.1 mm i.d., 5 μm pore size, Waters, Saint-Quentin en Yvelines) was used. An isochratic mobile phase was used consisting of water–acetonitrile (40:60, v/v), with a flow rate of 0.25 ml/min. The mobile phase was continuously degassed during experiments and the temperature was kept constant at 20 °C. Prior to injection to the column, a 200 μl sample of NP suspension was diluted with methanol (2 ml), sonicated for 5 min and filtrated through a 0.20 μm syringe filter (Supelco Minisart plus filters, Sigma–Aldrich). A 10 μl aliquot of the sample was injected. Retention time of tripentone was found to be 1.32 min and tripentone was detected at 259.8 nm with a photodiode-array detector. Two standard curves were prepared by plotting a known concentration of tripentone against the corresponding peak height or the corresponding peak area. In both case, these calibration curves for the quantification of tripentone were linear over the range of concentrations used, from 200 ng to 0.1 mg/ml (0.67 μM to 0.34 mM); ($r^2 > 0.99$).

2.6. In vitro tripentone release studies

For the release studies, a dialysis method was used since centrifugation did not allow the separation of NP in an adequate time interval due to their small diameter (Lamprecht et al., 2002). Subsequently, 1 ml of drug loaded NP suspension was filled into a dialysis tube (pore size of 100,000 Da), and incubated in phosphate buffer (pH 7.4) containing 10% (v/v) drug-free NP under gentle magnetic stirring (250 rpm) at 37 °C. At appropriate intervals, 1 ml samples were withdrawn, assayed for drug release and replaced by 1 ml of fresh buffer. The amount of tripentone in the release medium was determined by HPLC. All measurements were performed in triplicate.

2.7. In vitro antiproliferative activity against L1210

L1210 cells were seeded in 96-well microplates at a density previously determined to maintain control cells in exponential phase of growth for the duration of the experiment, and to obtain a linear relationship between the optical density and the number of viable cells (Pierre et al., 1991). The plates were incubated with the tested compounds, i.e. free or encapsulated tripentone or blank NP, for 48 h (four doubling times). Prior to experiments, tested NP were filtrated on 0.22 μm. At the end of the incubation period, 15 μl of 5 mg/ml 3-(4,5-dimethylthiazol-2-yl)-2,5-diphenyltetrazolium bromide (MTT, Sigma Chemical Co., Saint Louis, MO, USA) was added to each well and the plates were incubated for 4 h at 37 °C. The medium was aspirated and the formazan was solubilized by 100 μl of DMSO. The optical density (OD) read at 540 nm was measured with a plate reader (Multiskan MCC, Labsystem) connected to a computer. The percentage of growth was calculated for each well: percentage growth = [(OD treated cells)/(OD control cells)] × 100. The percentages of tri- or hexaplicate growth were then averaged and plotted as a function of the concentration log. The IC_{50}

Table 1
Estimation of the solubility of the tripentone in Labrafac® or in an aqueous solution of Solutol® by means of HPLC measurements

Sample	Labrafac® [g]	Solutol® [g]	Tripentone® [g]	Water [g]	Percentage of drug solubilized
A	0.514	–	0.005	1.481	70 ± 10 in Labrafac®
B	–	0.423	0.005	1.481	55 ± 5

(concentration reducing by 50% the OD) was calculated by a linear regression performed on the linear zone of the curve. The IC_{50} value of blank NP is given in equivalent tripentone concentration. The IC_{50} value of tripentone loaded NP is based on the initial amount of tripentone encapsulated in the NP.

3. Results

3.1. Tripentone solubility studies

To study feasibility to formulate tripentone loaded nanocapsules by applying the phase inversion process developed by Heurtault et al. (2002a), without using of any additional adjuvant nor alcohol nor organic solvent, tripentone affinities for the excipients were determined. Thus, the drug was mixed either (A) with triglycerides (Labrafac®) or (B) with an aqueous solution of the surfactant (Solutol®) in proportions similar to the ones used in the formulation of blank nanoparticles (Table 1). In addition, three heating–cooling cycles (85–60 °C) were applied to A and B under gentle magnetic stirring.

At the end of experiments, for A, two distinct phases are visible at room temperature: one rich in Labrafac® and an aqueous phase. Solubilized tripentone was determined in each phase. From HPLC measurements, no tripentone is recovered in water, and 70 ± 10% of the initial tripentone amount is solubilized in triglycerides.

For B, 55 ± 5% of tripentone is solubilized in the aqueous Solutol® solution. Moreover, from DLS measurements (results not shown), micelles with a mean radius of 6.5 nm are present.

3.2. Interfacial tension measurements

Fig. 2 shows the adsorption kinetics obtained at the Labrafac®–Solutol® interface in absence (curve 1) and in presence of the tripentone in Labrafac® (curve 2, Trip.L) or in the aqueous Solutol® solution (0.1 M) (curve 3, Trip.S). In the case of the Labrafac®–Solutol® interface, the initial interfacial tension is 4.4 ± 0.2 mN/m. Then, one can observe a slight decrease of γ with time; an equilibrium interfacial tension value of 3.4 ± 0.1 mN/m is obtained after 1000 s. No significant difference in the adsorption kinetics is observed for Trip.L or Trip.S in comparison with the Labrafac®–Solutol® interface.

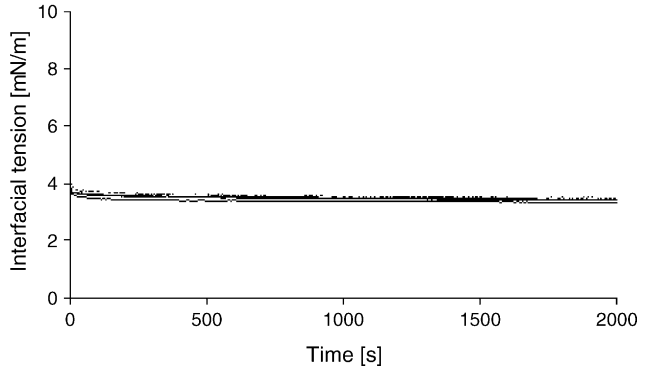

Fig. 2. Adsorption kinetics at the Labrafac®–aqueous Solutol® solution (0.1 M) interface: native interface ((1) ▬), adsorption kinetics of tripentone from Labrafac® [Trip.L] ((2) —) or from the Solutol® solution [Trip.S] ((3) . . .).

To more precisely characterize the organization of each interfacial film, its interfacial dilatational rheological properties were studied after adsorption kinetics reached an equilibrium state (typically ≈ 1000 s). Characteristic rheological parameters were determined using a modified Maxwell model (Table 2).

In absence of tripentone in the system, a pure elastic behavior is monitored for the Labrafac®–aqueous Solutol® solution and Ea is found to be 0.4 mN/m.

For Trip.L, a pure elastic behavior is observed and Ea is 0.3 mN/m.

For Trip.S, compression of interfacial layer is followed by a decrease of the surface pressure with time. This relaxation indicates a viscoelastic behavior. The relaxation curve is well-fitted with a monoexponentialmodel as indicated by the theoretical curve in Fig. 3A. The characteristic time is estimated to be 5.5 s. From another set of experiments performed at low rate of compression and by using our model, we deduced from the slope of the curve (Fig. 3B) the viscoelastic part of the elasticity (Ene = 0 mN/m), and from the value at the origin, the purely elastic part of the elasticity (Ee = 1.5 mN/m).

3.3. Formulation studies

In the formulation studies, tripentone was added to the mixture made by lipids, surfactants and water. The inversion phase process was then applied. Nanoparticles were obtained.

The average particle radius and polydispersity of different samples were determined from DLS measurements, by using both the method of cumulants and a Contin analysis and are listed in Table 3.

From the cumulant analysis of the data, blank and tripentone loaded NP hydrodynamic radii were determined to be about 29 and 28 nm, respectively. From the very low polydispersity index

Table 2
τ, Ee and Ene experimental values obtained at the Labrafac®–aqueous Solutol® solution (0.1 M) interface for the native interface, Trip.L and Trip.S

	Labrafac®–Solutol® (0.1 M)	Trip.L	Trip.S
Ee [mN/m]	0.4	0.3	1.5
Ene [mN/m]	–	–	0
τ [s]	–	–	5.5

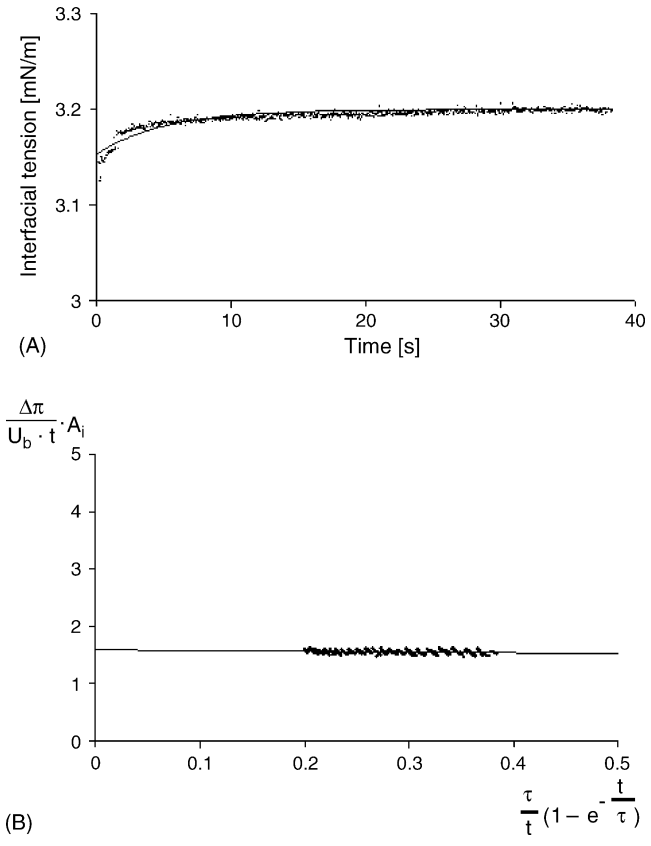

Fig. 3. (A) Typical results of the graphical determination of the characteristic time τ, experimental values (points) and theoretical values (solid line). The measurements were recorded during the fast compression of the Trip.S film at the Labrafac®–aqueous Solutol® solution (0.1 M) interface with a velocity of 2.7 s^{-1}. (B) Typical results of the graphical determination of Ee, the equilibrium part of the elasticity and Ene, the nonequilibrium part of the elasticity. The measurements were recorded during the slow compression of the Trip.S film at the Labrafac®–aqueous Solutol® solution (0.1 M) interface with a velocity of 7×10^{-3} s^{-1}.

(<0.03), one can consider that the particle size distribution is monomodal.

Particles radii were also determined from a Contin method. For blank NP, two populations appear: one with a mean peak value of 6.9 nm and another of 29 nm. The weight of the first population (0.004) is very small in comparison with the one of the second population (1.970). For tripentone loaded NP, only one peak appear with a hydrodynamic radius value of 28 nm.

To characterize the surface charge properties of nanoparticles, ζ-potential measurements were undertaken. A mean ζ-potential value of −8 mV was measured for blank NP and for tripentone loaded nanoparticles. The ζ-potential distribution profile of the two samples is shown in Fig. 4. For blank NP, two peaks are observed whereas only one peak is obtained for tripentone loaded NP.

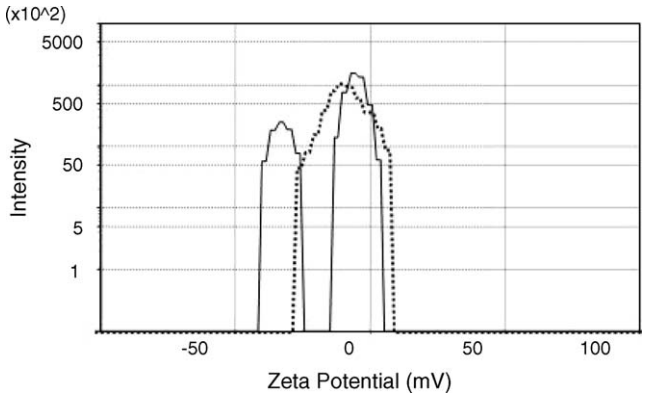

Fig. 4. ζ-Potential values obtained for blank nanoparticles (—) and tripentone nanoparticles (. . .) after 1:100 dilution in NaCl 1 mM (cell voltage of 150 V).

Fig. 5 shows transmission electron micrographs of the nanoparticles. For blank NP (Fig. 5A), a spherical shape can be observed for two populations of NP: one with a mean diameter of about 50 nm and another one with a mean size of about 13 nm. One can note the presence of a well-defined shell around the core of the NP. In the case of the tripentone loaded nanoparticles (Fig. 5B), only particles with an homogeneous size of about 50 nm can be observed. A little deformation of the form of the NP, from spherical to hexagonal, is visible for some NP. This modification of shape can be attributed to the evaporation process consecutive to the preparation and the analysis of the samples under vacuum. Nevertheless, in spite of the invasive imaging protocol of TEM, NP remain stable and structure of NP does not disrupt.

From HPLC measurements, the encapsulation efficiency of tripentone into NP was determined, and was found to be of 95% (Table 3).

3.4. In vitro release profile

In vitro tripentone release behavior is shown in Fig. 6. In phosphate buffer at pH 7.4, no drug release is detected within 3 days. This lack of release was also observed for amiodarone loaded lipid nanoparticles and was attributed in particular to the low drug solubility in the aqueous phase (Lamprecht et al.,

Table 3
Particle size and polydispersity index determined by the method of cumulants or a Contin method (results given as an unweighted distribution of the hydrodynamic radius, R_h), ζ-potential values and tripentone encapsulation recovery of the nanoparticles formulated

	Second-order cumulent analysis			Contin analysis						ζ-Potential [mV]	Encapsulation rate [%]
	R_h [nm]	Width	PDI	Peak I			Peak II				
				R_h [nm]	Relative width	Weight	R_h [nm]	Relative width	Weight		
Blank NP	28.52	3.67	0.017	6.91	±0.06	0.004	28.99	±0.16	1.970	−8.2 ± 2.2	–
NP + trip	27.48	3.35	0.015	–	–	–	27.89	±0.16	2.200	−8.1 ± 0.6	>95

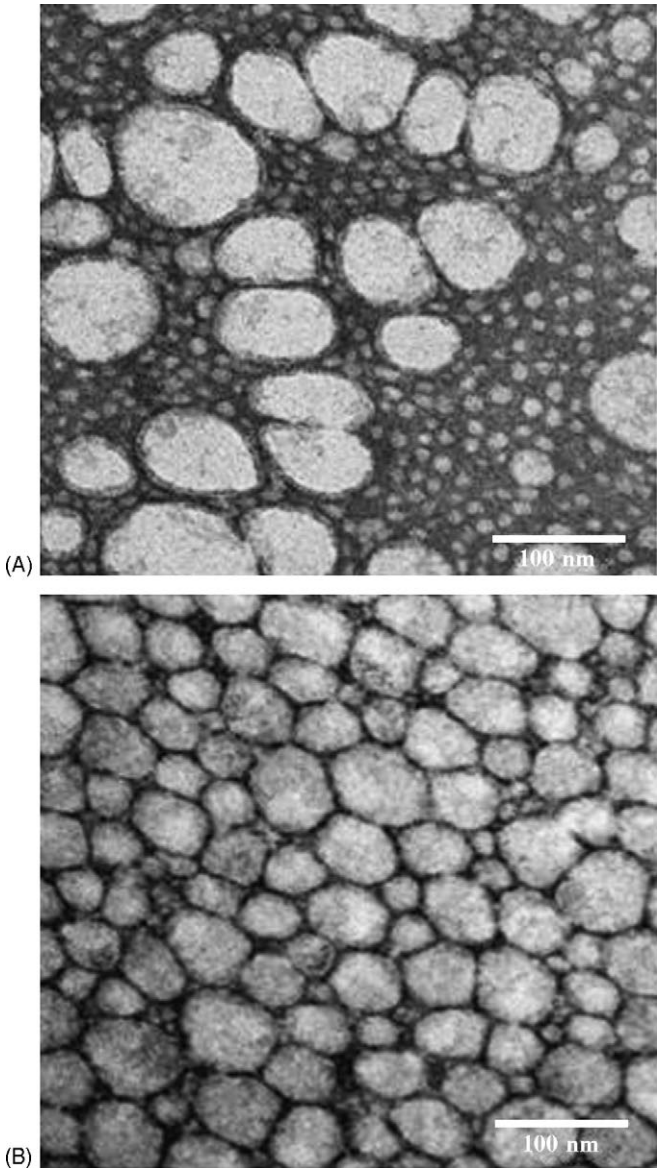

Fig. 5. Transmission electron micrographs of blank nanoparticles (A) and tripentone nanoparticles (B).

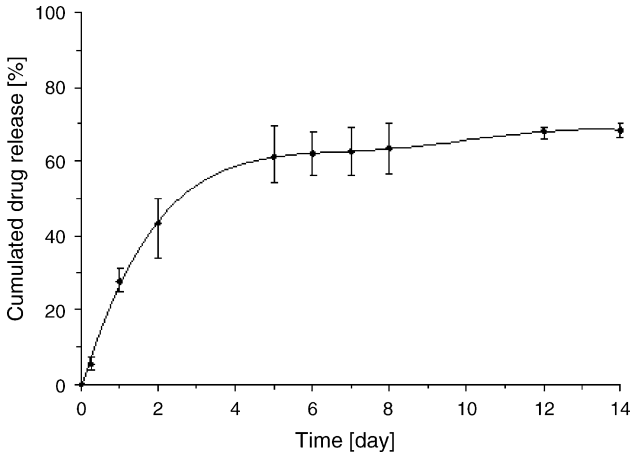

Fig. 6. In vitro release profile of tripentone from the lipid nanoparticles (blank nanoparticles as acceptor phase in phosphate buffer, pH 7.4, 37 °C).

Table 4
In vitro antiproliferative activity of free tripentone or tripentone loaded nanoparticles on L1210 cells

	Free tripentone	Blank NP	Tripentone NP
IC_{50} [μM]	0.015	1.5	0.014

2002). Addition of blank NP in the release medium was then considered. Indeed, to provide sink conditions, and in the same time, avoid the use of very large release volumes, a second compartment into the release medium can be used, acting as a kind of acceptor phase accumulating the drug from the release medium (Lamprecht et al., 2002). In presence of blank NP in phosphate buffer, one can observe a fast initial release of the drug in the first 2 days. After that, a sustained release of the encapsulated tripentone at a slower release rate can be observed and about 60% tripentone is released in 10 days.

3.5. In vitro antiproliferative study on L1210 cells

Table 4 shows IC_{50} results obtained in vitro for free tripentone, blank nanoparticles and tripentone loaded nanoparticles. For free tripentone, an IC_{50} value of 0.015 μM was determined. For tripentone loaded nanoparticles, an IC_{50} value of 0.014 μM was found. From that, no significant difference between free or encapsulated drug is found in in vitro tripentone cytotoxic activity on L1210 cells.

4. Discussion

The aim of the present work is to obtain lipid nanoparticles encapsulating a tripentone, a new antitubulin agent, by using a phase inversion process simple to use, not requiring any additional adjuvant, alcohol or toxic organic solvent.

By mixing tripentone with excipients and by applying the phase inversion process, nanoparticles were obtained. From DLS and TEM measurements, these nanoparticles present a very homogeneous size of about 50 nm. No significant difference of mean ζ-potential value is observed between blank and drug loaded nanoparticles. Thus, both nanoparticles samples would present a similar surface charge property, and tripentone would be well-encapsulated in nanocapsules with a high encapsulation efficiency above 95%.

From size measurements, TEM pictures and ζ-potential distribution profiles, it appears that two populations of blank NP coexist: a majority of NP with a size of about 50 nm, with a well-defined shell around the core of the NP, and a second population, very much in the minority, with a size of about 13 nm. Already in previous studies, the presence of two populations of blank lipid nanoparticles was supposed (Cahouet et al., 2002; Minkov et al., 2005). Indeed, from ζ-potential distribution profiles, surface tension and surface potential measurements, Minkov et al. (2005) assumed the coexistence of two blank NP populations: one very stable with a close pack Lipoid® monolayer around the Labrafac® core and another one less stable without Lipoid® molecules. Nevertheless, never before the present study, these two populations were directly observed.

On the contrary, in the case of tripentone loaded NP, only one population of NP is observed.

Equilibrium interfacial tension values obtained at the Labrafac®–Solutol® interface are in good agreement with those previously obtained by Heurtault et al. (2002b). Furthermore, very low Ee and Ene values are obtained. From adsorption kinetics and interfacial rheological results, it appears that when tripentone is dissolved in Labrafac®, molecules do not significantly adsorb at the created oil surface active agent interface but tend to stay in the oily volume. This result can be explained by the good affinity of the drug for triglycerides.

In conclusion, the fraction of tripentone initially present in Labrafac® in the formulation process would stay in the oily core of nanocapsules.

When tripentone is initially present in the aqueous Solutol® solution, no significant changes in adsorption kinetics are observed in comparison with the pure Labrafac®–Solutol® system: no tripentone molecules adsorb at the interface. Nevertheless, one can observe a change of the interfacial rheological behavior from elastic to viscoelastic, an Ene value of 0 mN/m, and a slight increase of the apparent elasticity. The value of Ene indicates no energetic dissipation, i.e. no expulsion of molecules upon compression towards the adjacent phases but the viscoelastic behavior implies a slower reorganization of the interface: the time required to reach a new equilibrium state after the constraint is increased in the presence of tripentone. The slight increase of Ee indicates a higher rigidity of the interfacial film. The concentration of Solutol® used in the formulation of NP is above the critical micellar concentration of the surfactant (Heurtault et al., 2002b). Therefore, interface structures would be micellar-like organizations in which tripentone could be incorporated. Solubility studies of tripentone in Solutol® are going in this way too.

The interpenetration of some tripentone molecules between those of Solutol® in the sublayers of the interfacial film could partially reorganize Solutol® at the interface and increase the hydrophilic in-between ethylene oxide units interactions. Indeed, the rigidity of the Labrafac®–Solutol® interface was attributed by Heurtault et al. (2002b) to interfacial hydrophilic in-between ethylene oxide Solutol® units interactions. Thus, the presence of tripentone helps to improve the cohesion of the interface.

Considering these different results, one can think that the majority of tripentone is solubilized in the NP oily core but some drug molecules interpenetrate surfactant units, and in particular the inner part of the nanocapsules shell since the mean ζ-potential value is unchanged between blank and drug loaded NP.

The interpenetration of tripentone molecules within Solutol® units can help to the stabilization of Solutol®. Indeed, by studying the electrokinetic properties of blank NP, Vonarbourg et al. (2005) showed that about 30% of Solutol® could be lost from the particle surface by dialyzing NP, then resulting in a better surface organization of the NP.

Tripentone stabilizing effect could help to the disappearance of the less stable blank NP population and to the formulation of a single stable tripentone loaded nanoparticles population.

Regarding the in vitro drug release profile, the initial tripentone release is probably due to drug molecules present in the NP shell. After this initial release phase, the drug release profile displayed may be attributed to the diffusion of NP oily core entrapped tripentone molecules.

The antiproliferative activities of the free and the encapsulated tripentone on L1210 cells were also determined. IC_{50} values well corroborate results previously obtained for the free drug on L1210 cells by Lisowski et al. (2004). The very low IC_{50} values confirm the strong cytotoxic activity of the tripentone. Moreover, IC_{50} values being unchanged between free tripentone and tripentone loaded NP, that proves that the activity of tripentone is totally recovered in vitro after encapsulation.

5. Conclusion

From results presented in this paper, it appears that nanoparticles of a new cytotoxic agent, a tripentone, homogenous in size, can be formulated according to a phase inversion process, simple to use and not requiring additional organic solvents. From different physicochemical characterization studies, tripentone would be well-encapsulated in the NP. Moreover, the presence of the drug in NP could help to the stabilization of the colloidal carriers. It was found that the drug release of the cytotoxic agent could be prolonged over a significant period, and the antiproliferative activity of the drug was totally recovered after encapsulation. The use of such colloidal carriers could help to improve the therapeutic efficiency of tripentone in the treatment of cancers, by delivering the incorporated drug to its action site.

Acknowledgments

The authors thank D. Goux for the TEM studies (Centre de Microscopie Electronique, University of Caen) and are grateful to A. Pierré and S. Léonce (Centre de Recherche Servier, Suresnes) for in vitro antiproliferative studies. S. Vrignaud was financially supported by Anvar (Aide aux Jeunes) of the Basse-Normandie (France).

References

Barnes, M.N., Grizzle, W.E., Grubbs, C.J., Partridge, E.E., 2002. Paradigms for primary prevention of ovarian carcinoma CA-cancer. J. Clin. 52, 216–225.

Boury, F., Ivanova, T., Panaiotov, I., Proust, J.E., Bois, A., Richou, J., 1995. Dilatational properties of adsorbed poly(D, L-lactide) and bovine serum albumin monolayers at the dichloromethane/water interface. Langmuir 11, 1636–1644.

Brigger, I., Dubernet, C., Couvreur, P., 2002. Nanoparticles in cancer therapy and diagnosis. Adv. Drug Deliv. Rev. 54, 631–651.

Cahouet, A., Denizot, B., Hindré, F., Passirani, C., Heurtault, B., Moreau, M., Le Jeune, J.J., Benoît, J.P., 2002. Biodistribution of dual radiolabeled lipidic nanocapsules in the rat using scintigraphy and γ counting. Int. J. Pharm. 242, 367–371.

Feng, S.-S., Chien, S., 2003. Chemotherapeutic engineering: application and further development of chemical engineering principles for chemotherapy of cancer and other diseases. Chem. Eng. Sci. 58, 4087–4114.

Gref, R., Domb, A., Quellec, P., Blunk, T., Müller, R.H., Verbavatz, J.M., Langer, R., 1995. The controlled intravenous delivery of drugs using

PEG-coated sterically stabilized nanospheres. Adv. Drug Deliv. Rev. 16, 215–233.

Heurtault, B., Saulnier, P., Benoît, J.P., Proust, J.E., Pech, B., Richard, J., 2000. Nanocapsules lipidiques, procédé de préparation et utilisation comme médicament. French Patent 0002688000.

Heurtault, B., Saulnier, P., Pech, B., Proust, J.E., Benoît, J.P., 2002a. A novel phase inversion-based process for the preparation of lipid nanocarriers. Pharm. Res. 19, 875–880.

Heurtault, B., Saulnier, P., Pech, B., Proust, J.E., Benoit, J.P., 2002b. Properties of Polyethylene glycol 660 12-hydroxy stearate at the triglycerides/water interface. Int. J. Pharm. 242, 167–170.

Heurtault, B., Saulnier, P., Pech, B., Venier-Julienne, M.C., Proust, J.E., Phan-Tan-Luu, R., Benoît, J.P., 2003. The influence of lipid nanocapsule composition on their size distribution. Eur. J. Pharm. Sci. 18, 55–61.

Hoarau, D., Delmas, P., David, S., Roux, E., Leroux, J.C., 2004. Novel long-circulating lipid nanocapsules. Pharm. Res. 21, 1783–1789.

Jemal, A., Murray, T., Ward, E., Samuels, A., Tiwari, R.C., Ghafoor, A., Feuer, E.J., Thun, M., 2005. Cancer statistics CA-cancer. J. Clin. 55, 10–30.

Lamprecht, A., Bouligand, Y., Benoît, J.P., 2002. New lipid nanocapsules exhibit sustained release properties for amiodarone. J. Control. Release 84, 59–68.

Lamprecht, A., Saumet, J.L., Roux, J., Benoit, J.P., 2004. Lipid nanocarriers as drug delivery system for ibuprofen in pain treatment. Int. J. Pharm. 278, 407–414.

Lisowski, V., 2002. Conception, synthèse, étude physico-chimique et évaluation biologique de "tripentones" à visée anticancéreuse. Ph.D. Thesis. Caen University.

Lisowski, V., Enguehard, C., Lancelot, J.C., Caignard, D.H., Lambel, S., Leonce, S., Pierre, A., Atassi, G., Renard, P., Rault, S., 2001. Design synthesis and antiproliferative activity of tripentones: a new series of antitubulin agents. Bioorg. Med. Chem. Lett. 11, 2205–2208.

Lisowski, V., Leonce, S., Kraus-Berthier, L., Sopkova de Oliveira Santos, J., Pierre, A., Atassi, G., Caignard, D.H., Renard, P., Rault, S., 2004. Design, synthesis and evaluation of a novel thienopyrrolizinone as antitubulin agents. J. Med. Chem. 47, 1448–1464.

Malzert, A., Boury, F., Renard, D., Robert, P., Proust, J.E., Benoit, J.P., 2002a. Influence of some formulation parameters on lysozyme adsorption and on its stability in solution. Int. J. Pharm. 242, 405–409.

Malzert, A., Boury, F., Saulnier, P., Benoit, J.P., Proust, J.E., 2002b. Rheological study of lysozyme and PEG2000 at the air–water and dichloromethane–water interfaces under ramp type or sinusoidal perturbations. Langmuir 18, 10248–10254.

Maulucci, G., De Spirito, M., Arcovito, G., Boffi, F., Castellano, A.C., Briganti, G., 2005. Particle size distribution in DMPC vesicles solutions undergoing different sonication times. Biophys. J. 88, 3545–3550.

Mc Guire, W.P., Markman, M., 2003. Primary ovarian cancer chemotherapy: current standards of care. Br. J. Cancer 89, 3–8.

Minkov, I., Ivanova, T., Panaiotov, I., Proust, J., Saulnier, P., 2005. Reorganization of lipid nanocapsules at air–water interface. I. Kinetics of surface film formation. Colloid Surf. B 45, 14–23.

Ozols, R.F., Bookman, M.A., Connolly, D.C., Daly, M.B., Godwin, A.K., Schilder, R.J., Xu, X., Hamilton, T.C., 2004. Focus on epithelial ovarian cancer. Cancer Cell 5, 19–24.

Panaiotov, I., Ivanova, T., Proust, J.E., Boury, F., Denizot, B., Keough, K., Taneva, S., 1996. Effect of hydrophobic protein SP-C on structure and dilatational properties of the model monolayers of pulmonary surfactant. Colloid Surf. B 6, 243–260.

Pierre, A., Krauss-Berthier, L., Atassi, G., Cros, S., Poupon, M.F., Lavielle, G., Berlion, M., Bizzari, J.P., 1991. Preclinical antitumor activity of a new vinca alkaloid derivative S12363. Cancer Res. 51, 2312–2318.

Rault, S., Enguehard, C., Lancelot, J.C., Robba, M., Atassi, G., Pierre, A., Caignard, D.H., Renard, P., 1998. Nouveaux dérivés de 8H-thieno[2,3-*b*]pyrrolizine-8-one, leur procédé de préparation et les compositions pharmaceutiques qui les contiennent. European Patent 9809552.

Saulnier, P., Boury, F., Malzert, A., Heurtault, B., Ivanova, T., Cagna, A., Panaiotov, I., Proust, J.E., 2001. Rheological model for the study of dilatational properties of monolayers comportment of dipalmitoylphosphatidylcholine (DPPC) at the dichloromethane (DCM)/water interface under ramp type or sinusoidal perturbations. Langmuir 17, 8104–8111.

Tewes, F., Boury, F., 2005. Formation and rheological properties of the supercritical CO_2–water pure interface. J. Phys. Chem. B 109, 3990–3997.

Vonarbourg, A., Saulnier, P., Passirani, C., Benoit, J.P., 2005. Electrokinetic properties of noncharged lipid nanocapsules: influence of the dipolar distribution at the interface. Electrophoresis 26, 2066–2075.

Ziller, C., Lincet, H., Muller, C.D., Staedel, C., Behr, J.-P., Poulain, L., 2004. The cyclin-dependent kinase inhibitor p21cip1/waf1 enhances the cytotoxicity of ganciclovir in HSV-tk transfected ovarian carcinoma cells. Cancer Lett. 212, 43–52.